

# AGAPEROS: Searching for variable stars in the LMC Bar<sup>\*</sup>

## II. Temporal and near-IR analysis of Long-Period Variables

T. Lebzelter<sup>1</sup>, M. Schultheis<sup>2</sup>, and A. L. Melchior<sup>3</sup>

<sup>1</sup> Institut für Astronomie, Türkenschanzstr. 17, A-1180 Wien, Austria

<sup>2</sup> Institut d'Astrophysique de Paris, CNRS, 98bis Bd Arago, 75014 Paris

<sup>3</sup> LERMA, Observatoire de Paris, 61 av. de l'Observatoire, 75014 Paris, France

Received .... / Accepted .. .....

**Abstract.** We analysed the light curves of a large sample of long period variables in the LMC from the AGAPEROS catalogue. The (non)regularity of the light change is discussed in detail showing that the majority of the light curves cannot be described properly by a single period. We show that semiregular and small amplitude variability do not necessarily correlate as has been assumed in several previous studies. Using near-infrared data from the DENIS survey we correlate the light change with colours and luminosities of the objects. These results are used to compare long period variables in the LMC with LPVs in the Galactic Bulge and in the solar neighborhood.

**Key words.** stars: variable: general - infrared: stars - Magellanic Clouds - stars: AGB and post-AGB

### 1. Introduction

The late stages of stellar evolution are characterized by regular and irregular light variability, a well-known signature of the stellar pulsation of Asymptotic Giant Branch stars (hereafter AGB). These light changes allow to identify AGB stars over large distances and to derive the pulsation characteristics (periodicity, etc.), which are key parameters for understanding the fundamental properties of the highly extended atmospheres of these stars. The pulsational properties have a strong impact on the structure of AGB stars. Pulsation, as the driving mechanism for the stellar winds, plays a key role for the high mass loss rates reached during the AGB phase.

A new era in the study of variable red giants started, when microlensing surveys produced a large amount of light curves of these stars, especially for objects in the LMC. The pioneering work by Wood (2000), using data from the MACHO survey, showed that the red giant variables form four roughly parallel sequences in a period-magnitude diagram. Three of these sequences could be associated with fundamental, first and second overtone pulsation. The explanation of the fourth sequence is not clear yet (Wood 2000, Hinkle et al. 2002). Recently, Cioni et al. (2001) presented a survey of variable red giants in the LMC based on data from the EROS-2 microlensing survey (Lasserre et al. 2000). The work of Cioni et al. focused

on the logP–K relation confirming three of the relations found by Wood, and they discussed the behaviour of different groups of variables in near infrared colour-magnitude diagrams.

The present paper relies on the variability information contained in the AGAPEROS variable star catalogue (Melchior et al. 2000). Here, we extend and analyse the corresponding light curves, relying on the EROS-1 microlensing survey data set (Ansari et al. 1995, Aubourg et al. 1995). These data have been obtained between December 1991 and April 1994. The second half of the data set therefore overlaps with the MACHO survey. We combine the EROS data with IJK<sub>S</sub> photometry of the DENIS survey (Epchtein et al. 1997), with an approach similar to the work of Cioni et al. 2001. The intention of our work is to discuss the light change of red variables on a large and homogeneous sample and to compare the results for LMC red variables with the corresponding objects in the Galactic Disk and Bulge.

### 2. Data

We have studied the AGAPEROS catalogue of 584 variable stars detected over a 0.25 deg<sup>2</sup> field in the LMC Bar (Melchior et al. 2000, hereafter referred to as Paper I). These stars have been selected on the basis of their variability on a 120-days window with a bias towards long-timescale variations (> few days), which are not necessarily periodic. The original data set has been taken at ESO by the EROS-1 collaboration (Arnaud et al., 1994a,b,

Send offprint requests to: schulthe@iap.fr

<sup>\*</sup> This work is based on data collected by the EROS and DENIS collaborations.

Renault et al. 1997) using a 40cm telescope, equipped with a wide field camera composed of 16 CCD chips, each of 400×579 pixels of 1.21 arcsec (Arnaud et al. 1994b). We use 9 chips, and study light curves in the red ( $\bar{\lambda} = 670\text{nm}$ ) filter. Table 1 gives a short description of the dataset. See Melchior et al. (1998,1999) for a more detailed description of the data treatment.

The study of the position of these stars in the colour-magnitude diagram showed that this catalogue is dominated by a population of Long Timescale & Long Period variables, while a few “bluer” variables have also been detected. A cross-correlation with various existing catalogues showed that about 90% of those variable objects were undetected before. We extended the corresponding light curves to the whole EROS-1 database of the LMC (900-days). We improved the photometry of the corresponding light curves with image subtraction using the ISIS2.1 algorithm of Alard (2000). We follow the same definition of the magnitude system as in Paper I, but we rely here on image subtraction photometry.

**Table 1.** Description of the dataset

time range (JD)	2448611 - 2449462
seasonal gaps	2448721 - 2448860 2449076 - 2449207*
mean number of data in each light curve	448
mean sampling	1.6 days

\* 54 light curves have a larger gap of 482 days.

The published DENIS catalogue (I, J and  $K_s$ ) for the LMC (Cioni et al. 2000) has been used to make a cross-identification between the AGAPEROS variables and the DENIS magnitudes. A search radius of 3'' was chosen to avoid misidentification. Out of the 584 variables 468 were detected by DENIS ( $\sim 80\%$ ). Note that the positional accuracy of these variables is about 1'', as discussed in Paper I.

### 3. Classification of the variables

Classically, three types of variable red giants have been defined (General Catalogue of Variable Stars, GCVS, Kholopov et al. 1985-88): Mira-type variables show periodic large amplitude variations with time scales typically of the order of 200 to 500 days. Semiregular variables (SRVs) show a less regular behaviour and a smaller amplitude. A typical time scale of the variation can be found, but the light curve shows phases of irregularity as well. The GCVS has introduced a limiting amplitude of 2.5 mag to separate Miras and SRVs. While even within the GCVS this rule has not been strictly applied (see e.g. the SRV W Hya), several investigators used this simple criterion for classification (e.g. Alard et al. 2001, Cioni et

al. 2001). The artificial nature of this division has been criticized already e.g. by Kerschbaum (1993). The third group of variables are the irregular variables. It is still not clear if such stars really exist or if these objects are simply not observed well enough to detect the same amount of periodicity as in the SRVs (e.g. Lebzelter et al. 1995).

In this work, we used a different approach to classify the light curves of the red giants in our sample. The classic classification system depends on whether a more-or-less constant period can be found and also depends on an arbitrary amplitude limit. Here we adopt a new scheme which is based on how well the light curve can be described by one or two periods only and where amplitude plays no role. In this way we are able to separate the two effects amplitude and regularity.

We based the classification on the regularity of the light curve on a visual comparison of the light change with a combination of up to three sine curves. To derive the periods, a Fourier analysis of the light curves (based on the program Period98 by Sperl (1998)) has been applied. Semiregular and irregular light changes result in a large number of peaks of similar strength in the Fourier spectrum (Lebzelter 1999, see below). Therefore the periods used for the fit have been selected from peaks in the periodogram by visual inspection. The amplitudes of the peaks were the starting point for the selection of the periods. Naturally, this selection is influenced by aliases. Fig.2 shows the typical spectral window of our data that has been used to identify spurious peaks. The selected periods were always cross checked by a visual comparison with the light curve. For unclear cases a second Fourier analysis was made with the primary period subtracted.

As a first approach to this large amount of light curve data we made no attempt to fit every detail of the light curves but identified the major period(s) to roughly resemble the overall light change. A more detailed fitting, as it was done by e.g. Kerschbaum et al. (2001) for a small number of SRVs in the solar neighborhood, is planned. Finally, we stress that the total available baseline of the data set did not allow to derive periodicities on time scales longer than 900 days. The classification is based on three years of observation and represents the behaviour of each object over the 900-days window. Stars classified as *irregular* may show some periodicity on a longer time scale or during a different time interval. The amplitudes were estimated visually from the lightcurve.

We classified the light curves on the regularity and type of their light change into four groups:

- *Regular*: A constant cycle length is observed for the available measurements. Some of these objects show some amplitude variations or bumps in their light curves. This group includes also stars which show a second period, if the two periods allow a very good fit of the light curve. While this group will include almost all objects that classically would have been classified as Miras, possible small amplitude regular variables will be found in this class as well. We therefore did not

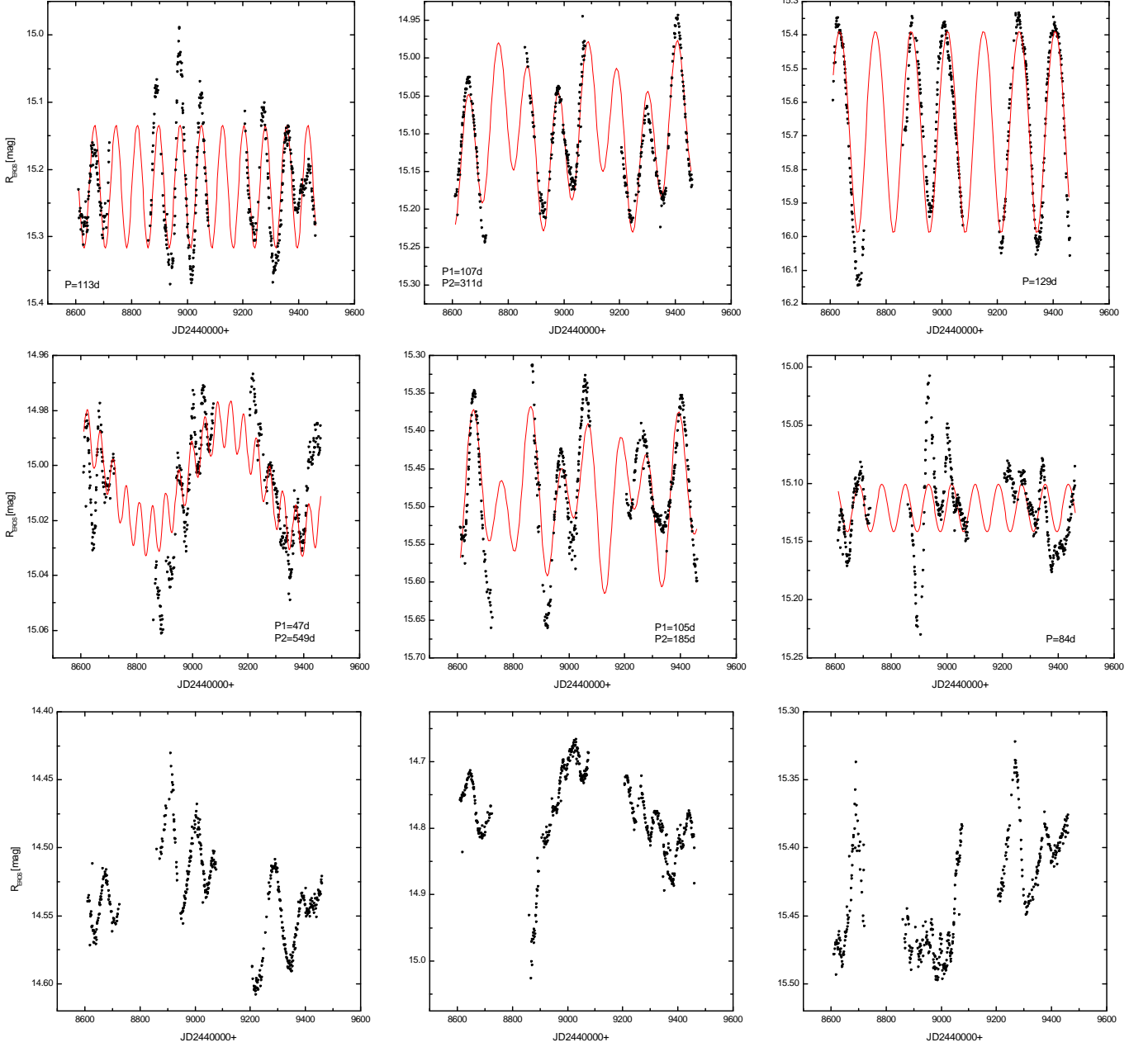


**Fig. 1.** Example light curves for each group of variables: The upper row illustrates regular light variation, the middle panels shows representatives of the semiregular variables, and the bottom row gives light variations classified as irregular. Periods used for the fit are given in the plot. The amplitudes ( $\Delta R_{\text{EROS}}$ ) are given in mmag

use the name "Miras" for this group. The only regular pulsators we did not include here were cepheids and obvious binaries, which have been classified as *Other*.

- *Semiregular*: The cycle length is variable, but some kind of periodicity is visible. The stars show up to three strong peaks in the Fourier spectrum. In some cases the light change can be fitted rather well with three or four periods.
- *Irregular*: These stars do not show any significant periodicity in their light change. Their light change occurs on time scales typical for AGB stars (i.e. a few 10 to a

few 100 days). Typically, the Fourier spectrum shows a large number of peaks with similar strength.

- *Other*: This group includes stars with a large fraction of bad data points, stars that turned out to be constant (misidentification due to some erroneous data points), and stars with a luminosity variation atypical for long period variables (including a number of binaries). A large fraction of these objects have also no DENIS data.

Fig. 1 shows a sample of regular, semiregular and irregular light curves. Note that our classification does not take into account the amplitude of the variation as in the

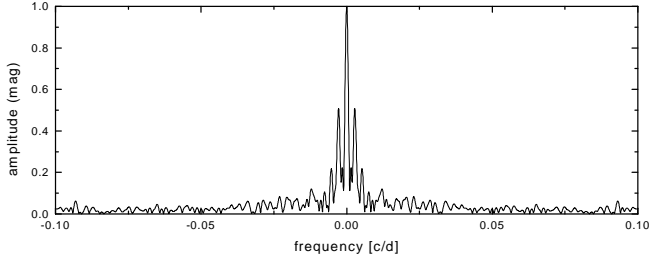


**Fig. 2.** Spectral window for the light curves used in this paper.

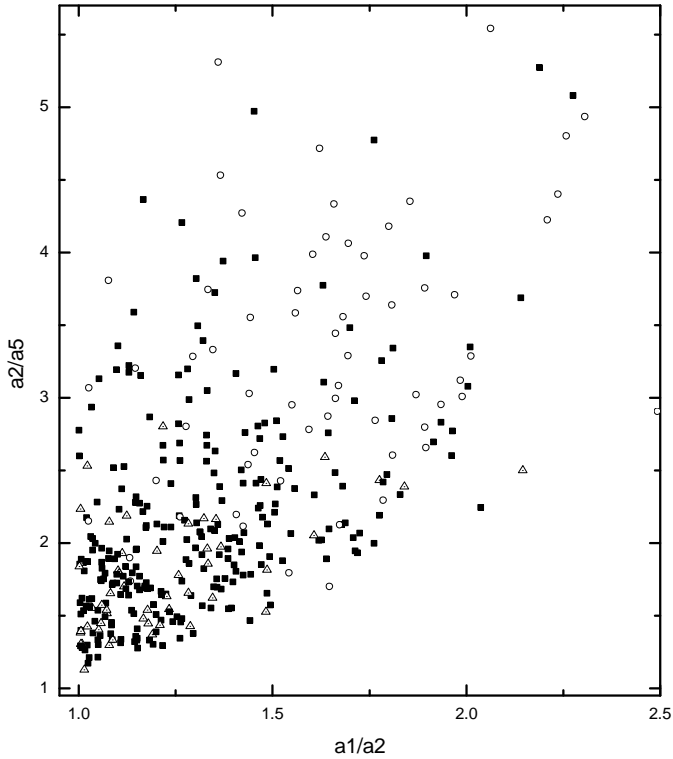


**Fig. 3.** Ratio of the two strongest peaks of the Fourier amplitude spectrum versus the ratio of the second and fifth strongest peak. Open circles denote regular variables, filled boxes indicate semiregular variables and open triangles mark irregular variables. A few objects found at even higher ratios are not included in the plot.

GCVS classification. The examples were selected to represent the different expressions of variability found in the three groups. Among the *regular* variables, we included examples of amplitude variations (top left in Fig. 1), variables with two periods (top middle) and classical Mira variables (top right).

Naturally, this classification remains somewhat subjective. However, we made an attempt to check the homogeneity of our classification by using the Fourier spectra of the light curves. In Fig. 3, we plot the amplitude ratio of the strongest and the second strongest peak against the ratio of the second and the fifth strongest peak. The advantage of our sample is that all light curves have a similar sampling and therefore a similar spectral window.

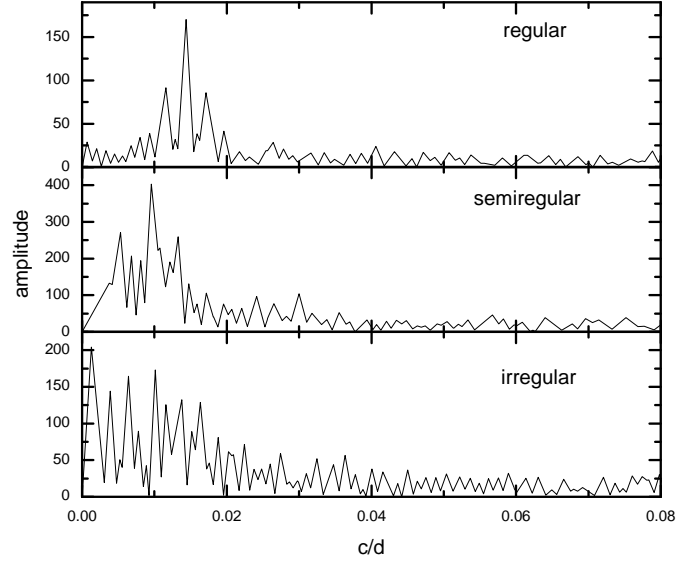


**Fig. 4.** Typical Fourier amplitude spectra for a regular, a semiregular and an irregular variable, respectively.

Examples for Fourier spectra and a spectral window are given in Fig. 4 and 2, respectively. A small number of stars has been excluded from this plot as their time coverage is not as good as for the majority of the sample.

As mentioned above, a semiregular or irregular light curve typically results in a number of peaks of similar strength in the Fourier spectrum. Stars classified as *regular* have only one or two strong peaks in their Fourier spectrum. They should therefore be found on the right-hand side and the top side of Fig. 3. Stars with a single period are on the right, stars with a second period in the upper left region of the plot. Note that there is no correction for aliases in this approach. From the spectral window (Fig. 2) one would expect to find stars with a single period at a ratio  $a1/a2$  of about 2.

For the *regular* variables the fifth strongest peak is typically already at the noise level and was used as a reference point. Note that we did not use more than three periods for each object in the following analysis. On the other hand, *irregular* variables should be found in the lower left corner of the plot. *Semiregular* stars are expected in between. Fig. 3 shows this classification indicated by different symbols.

We observe that our classification criteria is coherent within our sample. However, for an individual object, Fig. 3 is not usable for classification as the borders between the three classes are not well defined.

For each star classified as *regular*, *semiregular* or *irregular* a typical amplitude of the light variation was determined. In the case of semiregular and irregular variables the light amplitude can change dramatically. In these cases, we used a mean value of the variation. As no standard Johnson filters have been used a direct comparison of the amplitude values found here and those given in the GCVS or the MACHO catalogue is not possible.

#### 4. Comparison with results from the MACHO survey

We searched the MACHO Variable Star Catalogue (<http://www.macho.mcmaster.ca/Data/MachoData.html>) for variables within the fields covered by our sample and classified as LPV.WoodA, LPV.WoodB, LPV.WoodC and LPV.WoodD, respectively. The catalogue released on the web includes only a subsample of all variables found in the MACHO survey. It was therefore not surprising that we did not find all stars of our sample in the released MACHO catalogue, which is probably not complete in the area we are concerned with. In total, we found 36 MACHO LPVs that are within the fields we investigated. 25 of them had counterparts in our sample<sup>1</sup>. We assume that the remaining 11 stars are located on defects or borders of the CCD chips, but we did not investigate these objects further.

We applied the same analysis to the red MACHO light curves of these 25 stars. Results are listed in Table 2. The same classification was reached for 21 stars in our comparison, in two further cases either the MACHO or the AGAPEROS light curve was not of sufficient quality for the analysis. Interestingly, the two remaining objects with different classifications both show a higher degree of regularity in the MACHO data. In these cases our dataset was obviously not covering enough light cycles to reveal the regularity. We can estimate from this result that for less than 10% of the AGAPEROS light curves the regularity was not detected correctly.

22 of the LPVs in common with the MACHO catalogue agree in the main period within a few percent. The values we derived for the MACHO light curves are in good agreement with the results listed in the MACHO catalogue. However, the catalogue gives only one period for each object, so in cases we found multiple periods in our sample stars only one of them could be compared. Several of the secondary periods found in the AGAPEROS stars also agree quite well with values from the MACHO data. Very long periods could not be detected with the shorter time series of AGAPEROS data. The differences in some secondary periods illustrates the difficulty to derive a unique fit of these light curves with more than one period (see also Kerschbaum et al. 2001).

The good agreement in the classification between the AGAPEROS and the MACHO data, computed over independent data sets (1991-1994 for AGAPEROS, 1992-2000 for MACHO), strengthens the validity of our approach.

#### 5. General characteristics of the sample variables

*Semiregular* variables clearly dominate our sample of late type giants. 583 light curves have been analysed in total. 112 of them have been classified as *other*. Among the remaining 471 objects we classified 18% as *regular*, 67% as

<sup>1</sup> In the course of this comparison, we found that the star 78.5861.10/80.6466.5194 has two entries in the web based MACHO catalogue

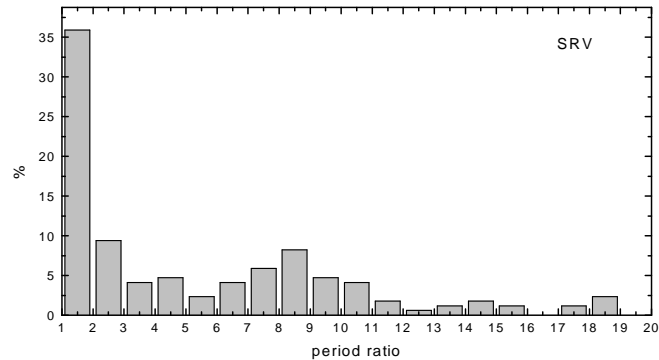


Fig. 5. Ratio between the short and the long period of semiregular variables with two periods.

*semiregular* and 15% as *irregular*. Due to different classification criteria a comparison of this result with other investigations is difficult. Cioni et al. (2001) found that 65% of the AGB stars are variable. As in our sample semiregular variables (in their case small amplitude red variables) are the dominant group of objects, only 12% of their stars have been classified as Miras.

If more than one period is detected, we have chosen a 'primary' period based on its amplitude. However, this decision is somewhat subjective when the amplitudes are similar. "Second periods" are present in at least 54% of the stars classified as *semiregular* and about 18% of the *regular* variables. For the *semiregular* variables the ratio between the short and long period is between 1 and 2 for about 36% of the objects (Fig. 5), the other *semiregulars* have period ratios between 2 and 15. This result is similar to what has been found in previous investigations of SRVs in our Galaxy (e.g. Kiss & Szatmary 2000). Among the *regular* variables with two periods about one third of the stars show a period ratio below 2.

Comparing amplitude with period shows a maximum amplitude for periods between 300 and 400 days, given our 900-day window. No large amplitude variables with periods below 100 days have been found. Details are illustrated in Fig. 6 where the mean amplitude has been calculated for each period bin. Alard et al. (2001) found a similar increase of mean amplitude from small to long periods in a sample of AGB variables in the Galactic Bulge. However, their sample shows a maximum amplitude at periods around 250 days, as they excluded all miras from their analysis. Fig. 7 summarizes the amplitude distributions within each class of variables. All three classes are dominated by small amplitude objects. Large amplitude stars occur exclusively among *regular* variables, all *irregular* objects are small amplitude stars.

We will now mainly concentrate on regular and semiregular variables. Fig. 8 shows the period distribution of the AGAPEROS sample. Both groups of objects (regular and semiregular) show a maximum at the shortest periods: Therefore, the *regular* variables cannot be simply related to the class of Mira variables. No Galactic Mira with a period below 100 days is known. Furthermore,

**Table 2.** Comparison of MACHO and EROS data

F.T.S. number	MACHO		Classif.	AGAPEROS		
	Period 1	Period 2		Period 1	Period 2	Classif.
77.7549.37	(74 d)		bad data*	77 d		semireg.
77.7550.65	593 d	77 d	regular			irreg.
77.7671.284	343 d		semireg.	346 d	39 d	semireg.
78.5616.19	68 d	73 d	semireg.	67 d	82 d	semireg.
78.5737.16	120 d		regular	119 d		regular
78.5737.19	346 d	3884 d	regular	340 d		regular
78.5739.75	96 d		regular	98 d		regular
78.5861.76	287 d	160 d	semireg.			bad data
78.5981.182	193 d		regular	189 d		regular
78.5978.71			irreg.			irreg.
78.6099.145	128 d		regular	129 d		regular
78.6223.71	352 d		semireg.	338 d	52 d	semireg.
78.6343.57	128 d		regular	128 d		regular
78.6345.14	239 d	126 d	semireg.	225 d	120 d	semireg.
78.6345.30	130 d		regular	129 d	236 d	regular
78.6461.2171	437 d	58 d	semireg.	454 d	51 d	semireg.
78.6466.18	338 d		regular	327 d		regular
78.6583.23	338 d		semireg.	345 d	56 d	semireg.
78.6586.61	121 d		regular	125 d	67 d	semireg.
78.6707.35	89 d		regular	88 d		regular
78.6824.2327	150 d		semireg.	150 d	315 d	semireg.
78.6826.70	86 d		regular	86 d		regular
79.5863.25	91 d	1143 d	semireg.	92 d	274 d	semireg.

\* The blue MACHO data give a period of 74 days.

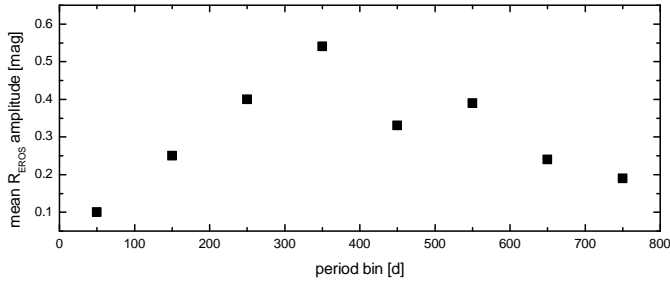


**Fig. 6.** Mean amplitude for each period bin. Only the primary period has been used in this plot.

Miras typically show large amplitude variability while the short period *regular* stars in our sample all have small amplitudes. The "classical" Miras probably form the second maximum in period distribution of the *regular* variables around 350 days, similar to the Galactic Miras. We conclude that the group classically known as semiregular variables may contain a substantial number of periodic variables. On the other hand it is known from long time series of Galactic semiregular variables that these stars can show phases of periodic behavior, so that these stars may exhibit semiregular behavior on longer time scales.

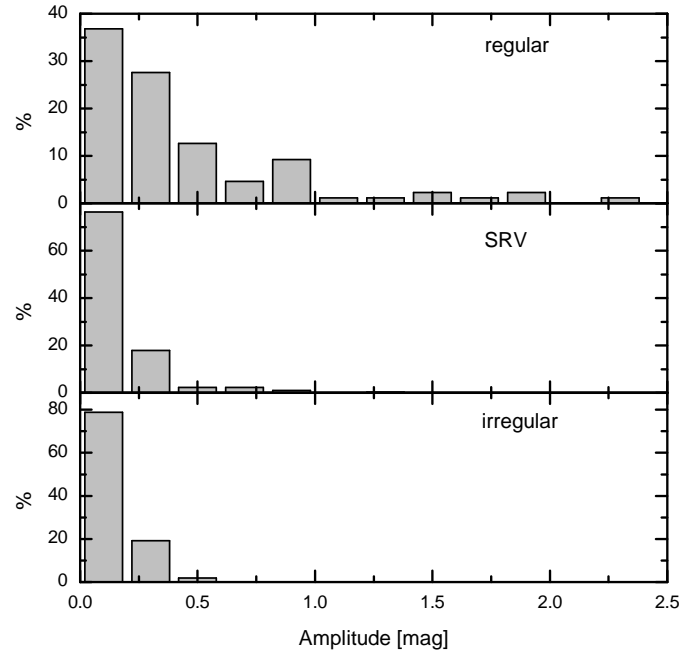


**Fig. 7.**  $R_{EROS}$  amplitude distribution for regular, semiregular and irregular variables, respectively. As discussed in Sect. 3, the amplitudes are estimated visually from the light curves.

## 6. Near-Infrared data

The near-infrared data from the DENIS survey allow to characterize the variables of our sample in more detail con-

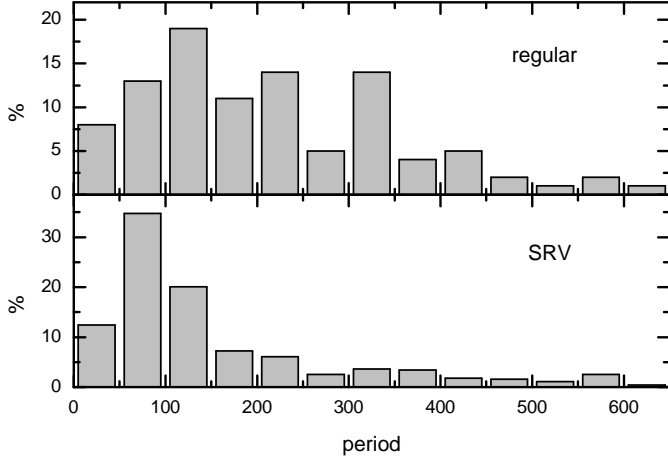


**Fig. 8.** Period distribution of regular and semiregular AGAPEROS variables. If a star has two periods, both have been included. Periods are given in days. The period determination is based on Fourier analysis as discussed in Sect. 3.

cerning their luminosity and chemical composition. Fig. 9 shows the  $K_S/(J - K_S)$  diagram for the AGAPEROS variables. One can clearly see that the majority of the sources are located above the tip of the Red Giant Branch (hereafter RGB-tip) which is for the LMC about 12.0 mag in  $K_S$  (Cioni et al. 2000a). We find regular and semiregular variables which are below the RGB-tip. These objects have rather short periods ( $< 100$  days) and could be AGB stars in the early evolutionary phase (early-AGB phase) or variable stars on the red giant branch.

Carbon-rich objects are characterized by their red ( $J-K$ ) and ( $I-J$ ) colour compared to the oxygen-rich sequence (see Cioni et al. 1999). However, as noted by Loup et al. (2002) the colour-colour diagram is just a statistical tool to distinguish between oxygen-rich and carbon-rich objects. Fig. 10 shows the  $(I - J)_0$  vs  $(J - K)_0$  diagram. Obviously, the ratio of regular to semiregular variables is smaller for the oxygen-rich stars than for the carbon-rich objects. This suggests that the majority of the semiregular variables are less massive than Miras which prevents them from becoming carbon stars.

We do not find any significant difference in colours or luminosities between SRVs with one single period and SRVs with multiple periods.

### 6.1. Colour-Period diagrams

For the LMC bar, it is obvious from Fig. 11 that the AGAPEROS variables follow a tight  $\log P$  vs  $I-J$  relation. It is important to emphasize that the  $I$  magnitudes of DENIS correspond to a *single* epoch measurement and thus the  $\log P$  vs.  $I-J$  diagram is affected by the scatter due to the amplitude variation of each source.

Relying on MACHO data in the Galactic Bulge, Schultheis & Glass (2001) demonstrated that semiregular variables in the Galactic Bulge show a noticeable scatter

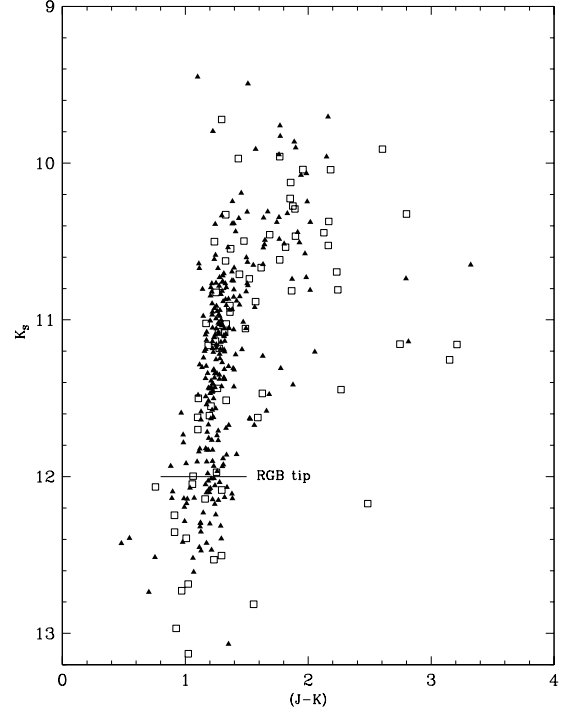


**Fig. 9.** Colour-magnitude diagram for DENIS/AGAPEROS stars. Regular variables are indicated by open squares, semiregular variables by filled triangles. The horizontal line indicates the tip of the red giant branch (RGB).

in  $I-J$  (3–4 mag) along the  $\log P$  vs  $I-J$  relation. The most significant difference between the Galactic Bulge and the LMC is the smaller range in  $I-J$  for the LMC ( $\sim 2$  mag) than for the Bulge ( $\sim 4$  mag). (see Fig. 11)

The  $I$  band for  $M$  stars is mostly affected by the strong  $\text{TiO}$  and  $\text{VO}$  molecular absorption (Turnshek et al. 1985, Lancon & Wood 2000). Schultheis et al. (1999) showed that lower metallicity is correlated with weaker  $\text{TiO}$  band intensities, corresponding to bluer  $I-J$  colours. The large scatter and the wide  $I-J$  range in the Galactic Bulge sample compared to the LMC might be explained by the wide spread in metallicity compared to the Magellanic Clouds. However, the difference in the  $I-J$  range between the Galactic Bulge ( $1 < (I - J)_0 < 5$ ) and the LMC ( $1 < (I - J)_0 < 3$ ) seems rather large. A more detailed quantitative analysis, using realistic model atmospheres of AGB stars (including metallic lines), is necessary to fully understand this systematic difference in the  $I-J$  colour between the Galactic Bulge and the LMC.

Fig. 12 displays the  $J-K$  colours of the AGAPEROS variables as a function of their period. The majority of the SRVs appear to follow a different period-colour relation with a slope flatter than the regular variables. For comparison, we indicated in Fig 12 the averaged colours of oxygen-rich Miras for the SgrI field (Glass et al. 1995). The majority of our long-period Miras ( $\log P > 250^{\text{d}}$ ) follow the location of the oxygen-rich Miras in SgrI. The

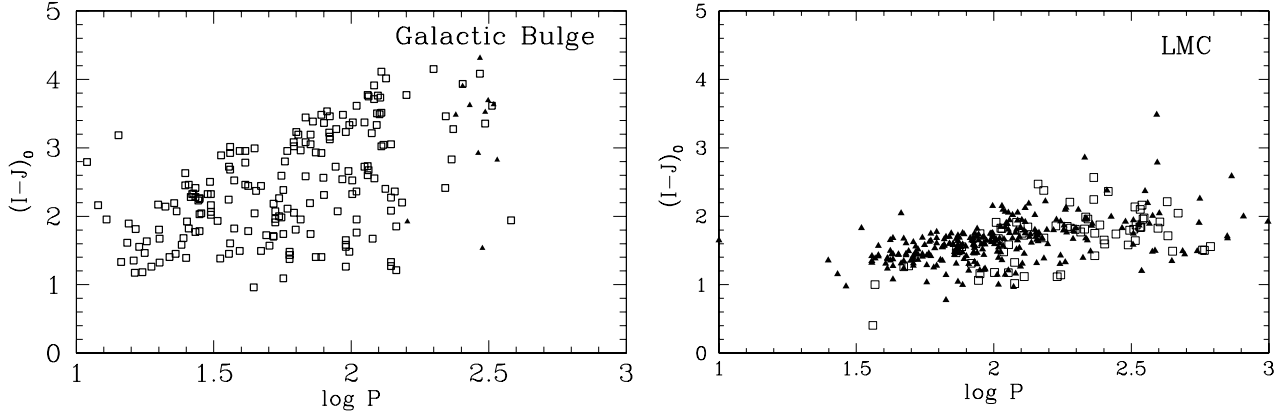


**Fig. 11.** LogP vs (I-J) relation for MACHO variables in Baade’s window (Schultheis & Glass 2001) compared to AGAPEROS variables in the LMC. The open squares on the left panel indicate the SRVs, while the filled triangles the Mira variables. On the right panel, same symbols as in Fig. 10. The periods are given in days.

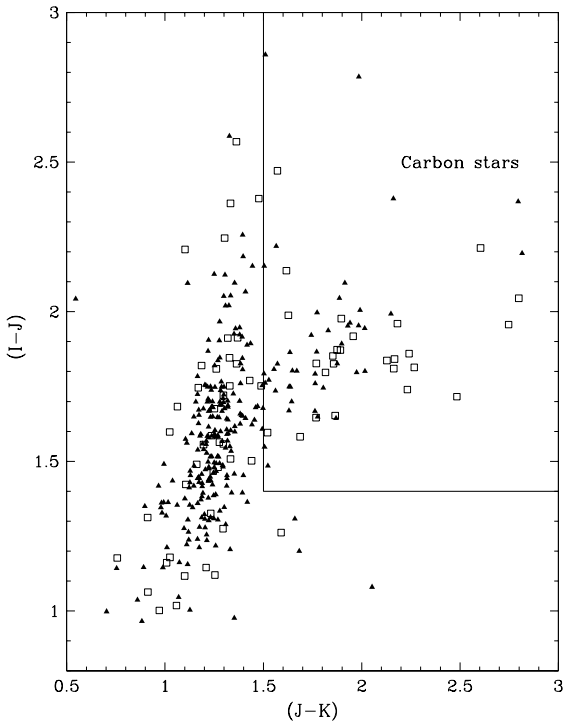


**Fig. 10.** DENIS colour-colour diagram for AGAPEROS variables. The box indicates the approximate location of carbon-rich objects (see Loup et al. 2002). Regular variables and semiregular variables are indicated by open squares and filled triangles, respectively.

carbon rich objects ( $J-K > 1.6$ ) seem to form a parallel sequence to the oxygen-rich Miras, while the long-period SRVs ( $P > 300^d$ ) do show clearly another period-colour relation. These stars are located on the sequence D in Wood’s diagram (see Wood et al. 1999 and discussion below) and are SRVs with multiple periods. A few long-period Miras also follow this sequence. However, the scatter in this diagram increases for  $\log P > 2.3$  due to the contribution of the circumstellar dust shell arising from

mass loss. Schultheis et al. (1999) and Schultheis & Glass (2001) obtain similar results for semiregular variables in the Galactic Bulge (see their Fig. 8).

## 6.2. $K_S$ vs $\log P$ diagram

In the Large Magellanic Cloud, the Miras and the SRVs seem to form distinct parallel sequences C,B,A which have been identified by Wood (2000) as pulsators in the fundamental, first and the next two higher overtones, respectively. Wood et al. (1999) showed by comparison of observed periods, luminosities and period ratios with theoretical models, that Miras are radial fundamental mode pulsators, while semiregular variables can be pulsating in the 1st, 2nd or 3rd overtone, or even the fundamental mode. The pulsation mode derived by Whitelock & Feast (2000) from diameter measurements of Miras in the Milky Way suggests first overtone pulsation for Miras. However, observations of radial velocity variations of Miras (e.g. Hinkle et al. 1982) clearly favour fundamental mode pulsation (Bessell et al. 1996).

In Fig. 13, we distinguish between semiregular variables with one period and those having a second or even third pulsational period. The location of our regular variables is consistent with the PL-relation from Feast et al. (1989) and Wood’s sequence C corresponding to fundamental mode pulsation. However, a few regular variables are also found to be located on sequence B and A (first and second overtones according to Wood (2000)). The majority of the SRVs follow Wood’s sequence B although the scatter is rather large ( $\sim 0.5$  mag in  $K_S$  at a given period). The SRVs situated on sequence A show very low amplitudes ( $< 0.5$  mag in  $R_{EROS}$ ) and typically no secondary periods. While Cioni et al. (2001) found no objects on sequence A, we could clearly confirm the existence of this PL-sequence. On sequence B and C, we find both single periodic and multiperiodic objects. The occurrence of single or multiple periodic behaviour does not depend on the luminosity.



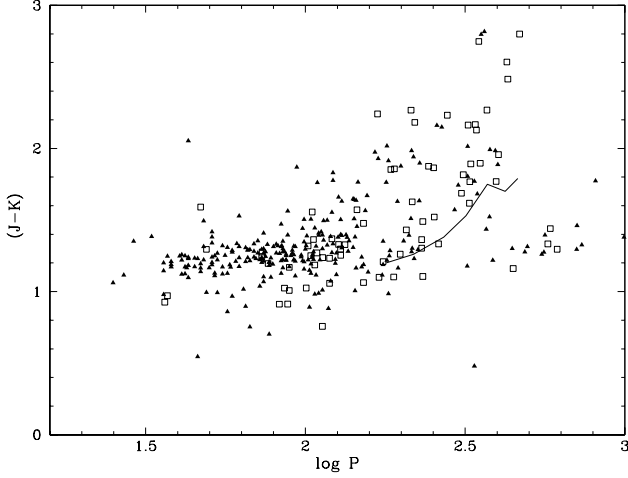


**Fig. 12.**  $\log P$  vs  $(J-K)$  relation for AGAPEROS variables in the LMC. The line indicates the average colours of Sgr I Miras for various period groups (Glass et al. 1995). The symbols are the same as in Fig. 10

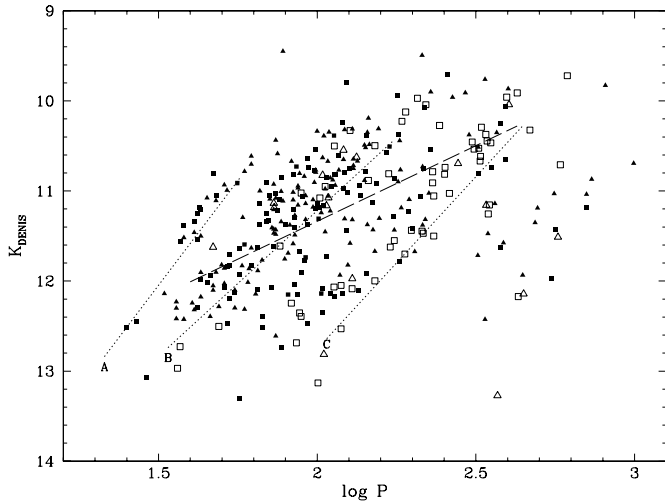


**Fig. 13.**  $K_S$  vs  $\log P$  diagram for AGAPEROS variables. The dashed line is the relationship suggested for local SRVs by Bedding & Zijlstra (1998). The dotted lines labelled A, B and C are eye fits to the sequence by Wood (2000). We use only the primary periods. Open squares show regular variables with one single period while regular variables with a second period are shown as open triangles. Semiregular variables with one single period are shown as filled squares while those with their second period are indicated as filled triangles. Sequence D of Wood (2000) lies on the right-hand side.

Several data points also mark sequence D of Wood (2000). The large scatter in this part of the  $K$ - $\log P$ -diagram is due to the limited time window of our data set. We are therefore able to reproduce all four sequences found in the MACHO data. The PL-relation for SRVs found by Bedding & Zijlstra (1998) from local objects could not be confirmed with our data (see below).

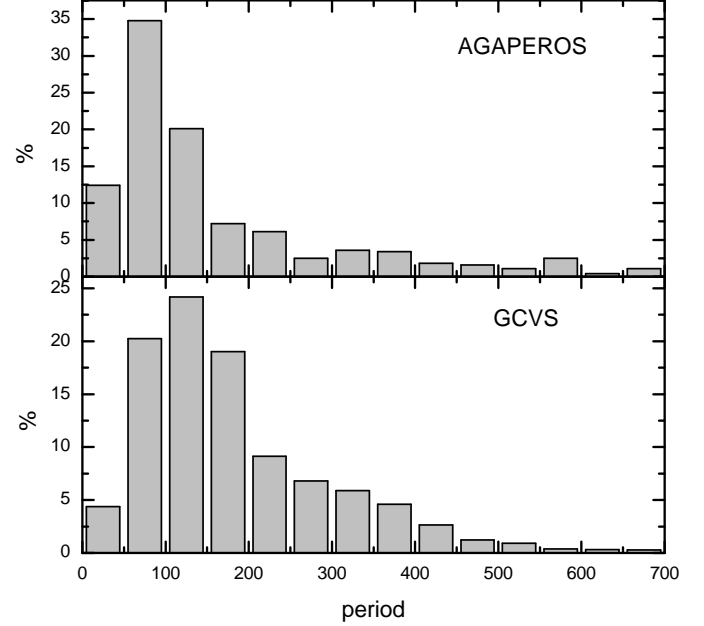


**Fig. 14.** Period distribution of semiregular variables in our sample and in the GCVS.

## 7. Discussion

### 7.1. Variability on the AGB

According to Fig. 9 most of the variables in our sample are on the AGB. Therefore, we can use our results to discuss the variability during the AGB phase. Our classification system for the type of variability aims to measure the regularity of the light change. Even not taking into account variations in the amplitude of the light change, we show that most stars have light curves that cannot be fitted by the simple combination of one or two excited periods. Regular variations are found with a wide range in period, while semiregular variability typically occurs mainly on time scales below 150 days (see Fig. 8). In Fig. 14, we compare the period distribution of the semiregular variables in our sample with the Milky Way SRVs listed in the GCVS. While in both cases the maximum of the distribution is at short periods, the GCVS distribution shows a significantly larger fraction of stars with periods longer than 150 days. These long periods may have been missed by our rather short time window. One would also expect a bias of the GCVS sample towards large amplitude variables as most of the data used there are based on photographic measurements. Furthermore, the period distribution from the GCVS given in Fig. 8 includes only one (main) period per object, while for the AGAPEROS data we give also secondary periods found for these stars.

Due to the separation of amplitude and regularity in our classification system, we can explore the relation between these two quantities. We find that large amplitude variation occurs almost exclusively among the *regular* variables (see Fig. 7). However, there exist *regular* pulsators with small amplitudes. It is therefore not correct to classify all red variables below a certain amplitude limit as

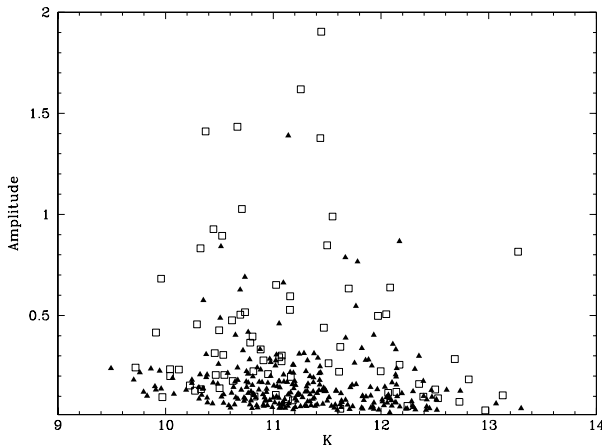


**Fig. 15.**  $R_{\text{EROS}}$  amplitude versus  $K_S$ . Open boxes denote *regular* variables, filled triangles *semiregular* stars.

semiregular. A division into large and small amplitude variables seems to be more meaningful. Large and small amplitude variables are both found all along the AGB. This is illustrated in Fig. 15 where the  $R_{\text{EROS}}$  light amplitude is plotted against the DENIS K band measurement. Towards the tip of the AGB the fraction of regular as well as large amplitude variables increases. Below the RGB-tip, amplitudes become on the average smaller. The occurrence of regular and semiregular as well as small and large amplitude variables on the AGB indicates that AGB stars have to be seen as a highly inhomogeneous group. One reason for this may be a difference in stellar mass as noted above.

Summarizing, large amplitudes are well correlated with regular pulsations, but we find no correlation between large amplitude and stellar luminosity nor between small amplitude variability and semiregularity of the light change. This result is in agreement with Wood et al. (1999).

## 7.2. PL-relation

In the literature, the observed PL-relation of long-period variables is considered to be the same in different environments such as the LMC, the Galactic Bulge or globular clusters (see e. g. Glass et al. 1995, Feast et al. 2002). It is therefore independent of metallicity, contrary to the predictions of pulsation theory (see e. g. Wood & Sebo 1996). However, previous studies were restricted to Mira variables mainly due to limitation of sensitivity. Thanks to the microlensing surveys such as EROS, MACHO or OGLE, we can study *systematically* small amplitude variations over a (still rather small) time interval. Wood (2000) found for the SRVs in the LMC different PL-relations for different pulsational modes. However, these separations cannot be reproduced in the Galactic Bulge (Schultheis & Glass 2001). In addition, the PL-relation of the solar neighborhood (Bedding & Zijlstra 1998) looks different. Why is

the PL-relation the same for Miras in different galactic environments, but *not* for SRVs?

Fig. 13 shows the PL-relation for the AGAPEROS sample. On the one hand, the Mira variables, classically defined as long period and large amplitude stars, concentrate along Wood’s sequence C. *Regular* variables at shorter periods would not have been classified as Miras. On the other hand, the semiregular variables (both according to the classical and to our definition), are spread all over the K-log P-plane. Making one fit with all *semiregular* stars would not result in a K vs. log P relation. In the solar neighborhood, Bedding & Zijlstra (1998) note that the SRVs are actually found on two sequences: the first one corresponds to the LMC Mira PL-relation (Wood’s sequence C); the second one is located close to a PL-relation derived from Galactic globular cluster LPVs shifted 0.8 mag from the Whitelock globular cluster sequence (Whitelock 1986), as shown in Fig. 13. The Bedding & Zijlstra sequence, defined for SRVs, obviously mixes objects from Wood’s sequence B and C, as shown in Fig. 13. The increase towards longer periods is consistent with the larger fraction of long period SRVs in the GCVS (Fig. 14) assuming that the detection of long periodic small amplitude variations is biased towards bright objects. Therefore, three PL-sequences seem to be more appropriate for semiregular variables. Multiperiodic stars are found on all three sequences A, B and C (see Fig. 13). Sequence D is almost exclusively occupied by stars with two periods in agreement with the suggestion from Wood (2000) that these long periodic variations are either due to binarity or a pulsation mode resulting from an interaction of pulsation and convection. However, there are also a few *regular* pulsating variables on this sequence with only one period. These stars would be definitely worth further investigation.

Schultheis & Glass (2001) showed that the interpretation of the PL-relation of Bulge SRVs is rather complex due to the depth of the Bulge ( $\sim \pm 0.35^{\text{mag}}$ , see Glass et al. 1995) and the variable interstellar extinction. There is no clear separation of the four sequences. We also showed that the LMC variables are much more homogeneous in their metallicity than the Bulge AGB stars (Fig. 11). This would explain part of the scatter in the K vs. log P plot for the Bulge.

## 7.3. Number densities

The number of semiregular variables in comparison to the regular variables is about a factor of 3. If we use the selection criterion of Cioni et al. (2001), i.e. all stars with  $R_{\text{EROS}}$  amplitudes smaller than 0.9 mag are SRVs, we end up with a ratio of almost 37 between SRVs and Miras in our sample. This value is much higher than what was found by Cioni et al. ( $\sim 5$ ), so we assume that our sample is more complete at smaller amplitudes. In the Galactic Bulge, Alard et al. (2000) found that the proportion of SRVs with respect to Miras is about a factor of 20. Most

recently, Derue et al. (2002) found a similarly large ratio between semiregulars and miras in the Galactic spiral arms. However, this ratio is of course very sensitive to the classification of SRVs (see above). For the Galactic disk, Kerschbaum & Hron (1992) found equal number densities for Miras and semiregular variables. However, they note that their sample of semiregular variables is probably not complete due to the difficulties in detecting small amplitude variables.

Do we see in different environments the same ratio of SRVs to Mira variables or does it depend on metallicity? Vassiliadis & Wood (1993) calculated lifetimes of the major evolutionary phases for different initial masses and different metallicities. They found that higher metallicity will increase the lifetime of the early-AGB but decrease the lifetime on the TP-AGB. Miras stars populate the TP-AGB, therefore in environments with higher metallicities, such as the Galactic Bulge the lifetime of the TP-AGB is shorter and thus the number densities should decrease. This might explain the correlation between the ratio of SRVs to Miras and metallicity. However, while a large fraction of our variables on the TP-AGB are *regular* variables<sup>2</sup> also *semiregular* variables are found. Lebzelter & Hron (1999) have shown that for stars in the solar neighborhood stellar evolution goes from SRVs to Miras. The *semiregular* stars found at a similar luminosity as the Miras (see Fig. 13) are therefore probably not in the same evolutionary state or they have different masses. Comparison of the number densities with expected lifetime is therefore problematic.

A lower metallicity leads also to a shift of the AGB towards higher temperatures in the HR diagram. The visual light change of these cool variables is dominated by highly temperature sensitive molecules like TiO (e.g. Reid & Goldston 2002). If the stellar temperature is higher, these molecules will play a minor role. Lower metallicity will also make the TiO bands weaker. Therefore one would expect that the visual amplitudes will in general be smaller for lower metallicity. This would favour small amplitude variability in metal poor environments and would explain the smaller fraction of large amplitude objects in the LMC compared to the Bulge. It would also be consistent with the complete lack of Miras in metal poor globular clusters (Frogel & Whitelock 1998).

However, one has to be extremely careful concerning possible selection effects, in particular for small amplitude variables. A homogeneous survey of variable stars in different Galactic environments is therefore needed.

*Acknowledgements.* ALM thanks the EROS collaboration and in particular Jean-Baptiste Marquette for his help with the light curves production with the image subtraction method. ALM is extremely grateful to Claude Lamy who performs the tremendous work of sorting the whole EROS-1 data set. TL has been supported by the Austrian Science Fund under project number P14365-PHY. MS is supported by the Fonds zur

<sup>2</sup> In this case *regular* variables and Miras can be assumed to be identical.

Förderung der wissenschaftlichen Forschung (FWF), Austria, under the project number J1971-PHY. We wish to thank Josef Hron for fruitful discussion. Finally, we wish to thank the referee for constructive comments. This paper utilizes public domain data obtained by the MACHO Project, jointly funded by the US Department of Energy through the University of California, Lawrence Livermore National Laboratory under contract No. W-7405-Eng-48, by the National Science Foundation through the Center for Particle Astrophysics of the University of California under cooperative agreement AST-8809616, and by the Mount Stromlo and Siding Spring Observatory, part of the Australian National University.

## References

- Alard, C., 2000, A&AS 144, 363  
 Alard, C., Blommaert, J.A.D.L., Cesarsky, C., et al., 2001, ApJ 552, 289  
 Alcock, C., Allsman, R.A., Alves, D.R., et al., 2001, ApJ 554, 298  
 Ansari, R., Cavalier, F., Couchot, F., et al., 1995, A&A 299, L21  
 Arnaud, M., Aubourg, E., Bareyre, P., et al., 1994, Exp. Astron. 4, 265  
 Arnaud, M., Aubourg, E., Bareyre, P., et al., 1994, Exp. Astron. 4, 279  
 Aubourg, E., Bareyre, P., Bréhen, S., et al., 1995, A&A 301, 1  
 Bedding, T.R., & Zijlstra, A.A., 1998, ApJ, 506, L47  
 Bessell, M.S., Scholz, M., & Wood, P.R., 1996, A&A, 307, 481  
 Cioni, M.R., Habing, H. J., Loup, C. et al., in “New views of the Magellanic Clouds, IAU symp. 190, p. 385  
 Cioni, M.R., Loup, C., Habing, H. J., et al., 2000, A&AS 144, 235  
 Cioni, M.R., van Marel, R. P., Loup, C., & Habing H. J., 2000, A&A 359, 601  
 Cioni, M.R., Marquette, J. B., Loup C., et al., 2001, A&A 377, 945  
 Derue, F., Marquette, J.-B., Lupone, S., et al., 2002, A&A 389, 149  
 Epchtein, N., de Batz, B., Capoani, L., et al. 1997, Messenger 87, 27  
 Feast, M.W., Glass, I.S., Whitelock, P.A., & Catchpole, R.M., 1989, MNRAS, 241, 375  
 Feast, M. W., Whitelock, P. W., & Menzies, J., 2002, MNRAS 329, L7  
 Frogel, J.A., & Whitelock, P.A., 1998, AJ, 116,754  
 Glass, I. S., Whitelock, P. A., Catchpole R. M., et al., 1995, MNRAS 273, 383  
 Hinkle, K.H., Hall, D.N.B., & Ridgway, S.T., 1982, ApJ, 252, 697  
 Hinkle, K.H., Lebzelter, T., Joyce R.R., & Fekel F.C., 2002, AJ 123, 1002  
 Kerschbaum, F., 1993, PhD thesis, Univ.of Vienna  
 Kerschbaum, F., & Hron, J., 1992, A&A 263, 97  
 Kerschbaum, F., Lebzelter, T., & Lazaro, C., 2001, A&A 375, 527  
 Kholopov, P.N., Samus, N.N., Frolov, M.S., et al., 1985-88, General Catalogue of Variable Stars. 4<sup>th</sup> edition, Nauka Publishing House, Moscow (GCVS)  
 Kiss, L.L., & Szatmary, K., 2000, IAU Symp. 191 ”AGB stars”, p. 133  
 Lançon, A., & Wood, P. R., 2000, A&AS 146, 217

- Lasserre, T., Afonso, C., Albert, J. N., et al., 2000, *A&A*, 355, L39
- Lebzelter T., *A&A* 351, 644
- Lebzelter, T., & Hron J., 1999, *A&A*, 351, 533
- Lebzelter, T., Kerschbaum F., & Hron J., 1995, *A&A* 298, 159
- Loup, C. et al., 2002, submitted to *A&A*
- Melchior, A.L., Afonso, C., Ansari, R., et al., 1998, *A&A* 339, 658
- Melchior, A.L., Afonso, C., Ansari, R., et al., 1999, *A&AS* 134, 377
- Melchior, A.L., Hughes, S. M. G., & Guibert, J., 2000, *A&AS* 145, 11
- Reid, M.J., & Goldston, J.E., 2002, *ApJ*, 568, 931
- Renault, C., Afonso, C., Aubourg, E., et al., 1997, *A&A* 324, L69
- Schultheis, M., Ng, Y. K., Hron, J., et al., 1998, *A&A* 338, 581
- Schultheis, M., Aringer, B., Jørgensen, U. G., Lebzelter, T., & Plez, B., 1999, in Hron, J., Höfner, S. (eds.), Abstract of the 2<sup>nd</sup> Austrian ISO workshop “Atmospheres of M,S and C Giants”, Vienna, Austria, 1999, p.93
- Schultheis, M., & Glass, I. S., 2001, *MNRAS* 327, 1193
- Sperl, M., 1998, *Comm. Asteroseismology (Vienna)* 111, 1
- Turnshek, D.E., Turnshek, D.A., Craine, E.R., & Boeshaar, P.C., 1985, *An Atlas of Digital Spectra of Cool Stars*, *A&AS Western Research Company*.
- Vassiliadis, E., & Wood, P. R., 1993, *AJ* 413, 641
- Whitelock, P.A., 1986, *MNRAS*, 219, 525
- Whitelock, P.A., & Feast, M., 2000, *MNRAS*, 319, 759
- Wood, P.R., 2000, *Proc Astr Soc Austr*, 17, 18
- Wood, P.R., & Sebo, K.M., 1996, *MNRAS*, 282, 958
- Wood, P.R., Alcock, C., Allsman R. A. et al., 1999, *IAU symp.* 191, p. 151